

# On the Product Formation in 1-Butene Metathesis over Supported Tungsten Catalysts

Liesel Harmse · Charl van Schalkwyk ·  
Eric van Steen

Received: 5 October 2009 / Accepted: 9 April 2010 / Published online: 22 April 2010  
© Springer Science+Business Media, LLC 2010

**Abstract** 1-Butene metathesis was performed over 8 wt% tungsten catalysts supported on silica, silica-alumina and  $\gamma$ -Al<sub>2</sub>O<sub>3</sub>. Under the applied reaction conditions, 1-butene metathesis yields with a relatively large selectivity iso-butene in addition to the expected metathesis products. The isobutene selectivity is high for catalysts with a relative low activity and decreases with increasing metathesis activity. It is deduced that iso-butene formation involves surface tungsten complexes, whose formation inhibits the metathesis activity.

**Keywords** 1-Butene metathesis · Tungsten · Silica-alumina

## 1 Introduction

Metathesis is a useful reaction to shift the composition of a pool of olefins to meet market demands. For instance, the Fischer-Tropsch synthesis produces a large amount of relatively low value butenes [1], which can be converted into higher value propene [2–4]. In particular, the cross-metathesis of butenes [4] is of interest, since it negates the loss of the valuable ethene in the production of propene. The cross-metathesis of 1-butene with 2-butene yields propene (with 2-pentene as a co-product) and the 1-butene

metathesis yields ethene and hexenes. The primary metathesis reaction can be defined as the conversion of 1-butene yielding ethene and *n*-C<sub>6</sub>-olefins and the conversion of 1-butene with 2-butene yielding propene and *n*-C<sub>5</sub>-olefins (i.e. assuming a rapid equilibration of the double bond isomerisation). The metathesis of butenes is equilibrium limited (see Fig. 1), and the equilibrium conversion of the C<sub>4</sub>-olefins in the primary metathesis reaction increases slightly with increasing temperature (from ca. 52 mol% at 300 K to 70% at 700 K). The maximum equilibrium yield of propene via the primary metathesis is obtained in the temperature range between 500 and 800 K (ca. 25.2 mol%). Higher propene yields can only be obtained by co-feeding ethene [6] representing a loss in the valuable ethene.

The higher thermodynamic yield of valuable chemicals in the metathesis of butenes demands the reaction to be carried out at relatively high temperature, thus necessitating the use of a tungsten-based catalyst. The use of WO<sub>3</sub>/SiO<sub>2</sub> for the metathesis of propene and butene is well documented [6, 7]. Huang et al. [3] obtained an improved performance of a supported WO<sub>3</sub>-catalyst in the cross metathesis of ethene with 2-butene by changing the support from  $\gamma$ -Al<sub>2</sub>O<sub>3</sub> to  $\gamma$ -Al<sub>2</sub>O<sub>3</sub>-HY. They attributed the enhanced performance to the change in the Brønsted acidity of the catalyst and a modification of the interaction between the tungsten species and the support. Similar results have been claimed for supported Re<sub>2</sub>O<sub>7</sub> metathesis catalysts [8, 9]. Higher turn-over frequencies have been obtained in Re<sub>2</sub>O<sub>7</sub>-catalysed metathesis using ordered mesoporous alumina (OMA) as a support material rather than conventional aluminas [10–13]. Supporting Re<sub>2</sub>O<sub>7</sub> on mesoporous silica, such as MCM-41, also results in more active catalysts than supporting on commercial silica [14]. Bakala et al. [15] argue that mesoporous materials as support materials for

L. Harmse · E. van Steen (✉)  
Department of Chemical Engineering, Centre for Catalysis  
Research, University of Cape Town, Private Bag X3,  
Rondebosch 7701, South Africa  
e-mail: eric.vansteen@uct.ac.za

L. Harmse · C. van Schalkwyk  
Sasol Technology Research & Development, P.O. Box 1,  
Klasie Havenga Road, Sasolburg 1947, South Africa

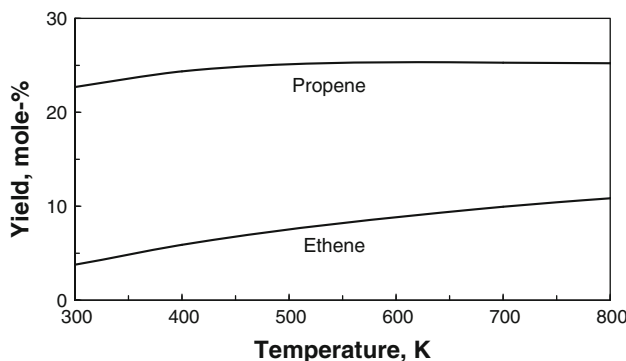


**Fig. 1** Equilibrium yield of propene and ethene in the metathesis of butanes considering double bond isomerisation, cross-metathesis of 1-butene with 2-butene and 1-butene metathesis (calculated with data from [5])

$\text{Re}_2\text{O}_7$ -based metathesis catalysts do not have a decisive advantage over commercial oxides, but that the challenge lies in obtaining a good dispersion of the active site.

The formation of propene via 1-butene metathesis requires double bond isomerisation activity of the catalyst, since only the cross metathesis of 2-butene with 1-butene yields the desired product (with  $\text{C}_5$ -olefins as a co-product). Brønsted acid sites are thought to be responsible for the required double bond isomerisation [16], but do not catalyse the metathesis reaction [17, 18].

The high reaction temperature of olefin metathesis may result in the formation of coke as was observed in the 1-heptene metathesis over  $\text{WO}_3/\text{SiO}_2$  [19]. Coke formation resulted in a decrease in the BET-surface area and the pore volume with a minimal loss in activity up to a coke content of the catalyst up to ca. 45 wt%. Formation of coke on metal oxide catalysed reactions is thought to be catalysed by the acid sites present within the catalyst [20]. Both Lewis acid sites and Brønsted acid sites may catalyse the formation of coke, the former by strongly interacting with basic species in the feed, and the latter via the normal carbocation route for coke formation [21].

Changing the acidity of the support may result in a change in the product composition obtained in the metathesis, and yield a better insight in the reactions occurring during olefin metathesis. In this study the product distribution in 1-butene metathesis is studied over a series of supported tungsten-based catalysts with different acidity with a view to gain a better understanding of the variety of products formed. Commercially available support materials were used in this study prepared by similar routes to study the effect of support acidity in the cross-metathesis of 1-butene, since acidic supports prepared by grafting alumina on mesoporous silica does not seem to enhance the catalytic activity significantly [15].

## 2 Experimental

### 2.1 Catalyst and Support Synthesis

Silica gel (Davisil grade 646, Aldrich), silica-alumina and alumina (Sasol Germany GmbH) were used as support material (see Table 1). The crushed support particles ( $d_{\text{particle}} = 300\text{--}500 \mu\text{m}$ ) were impregnated with an aqueous solution of ammonium metatungstate hydrate (Aldrich;  $[(\text{NH}_4)_6(\text{H}_2\text{W}_{12}\text{O}_{40})]_{\text{initial}} = 0.2778 \text{ mL dm}^{-3}$ ; pH: ca. 5) to yield an 8 wt%  $\text{WO}_3$ -loading on the support [22]. The slurry was stirred for 2 h at room temperature, after which the excess water was evaporated under reduced pressure (100 mbar) at ca. 373 K. The catalysts were dried in an oven at 383 K for 2 h. The temperature was then increased to 523 K at a rate of 1 K/min and kept at this temperature for 2 h. In the final step, the temperature was raised to 873 K at a rate of 3 K/min and maintained at this temperature for 8 h.

### 2.2 Support and Catalyst Characterization

The specific surface area and pore volume were determined for all the fresh and spent samples using  $\text{N}_2$ -physiosorption

**Table 1** Characteristics of support materials

Support material	Supplier	$\text{SiO}_2$ (wt%)	$\text{Al}_2\text{O}_3$ (wt%)	$S_{\text{BET}}$ ( $\text{m}^2/\text{g}$ )	$V_{\text{Pore}}$ ( $\text{cm}^3/\text{g}$ )	$d_{\text{Pore}}$ ( $\text{\AA}$ )	$d_{\text{Al}_2\text{O}_3}$ ( $\text{\AA}$ )	$n_{\text{acid}}^b$ (mmol/g)	$x_{\text{Lewis}}^c$	$k_{\text{db}}^d$ ( $\text{h}^{-1}$ )
$\gamma\text{-Al}_2\text{O}_3$	Sasol <sup>a</sup>	0	100	242	0.80	133	42	0.16	100	0.005
Siralox-20	Sasol <sup>a</sup>	20	80	351	0.70	80	39	0.22	97	0.118
Siralox-40	Sasol <sup>a</sup>	40	60	409	0.84	82	—	0.27	94	0.213
Siralox-75	Sasol <sup>a</sup>	75	25	339	0.31	37	—	0.25	72	0.143
$\text{SiO}_2$	Aldrich	100	0	300	1.15	149	—	0.01	—	—

<sup>a</sup> Sasol Germany GmbH

<sup>b</sup> Number of acid sites as determined using  $\text{NH}_3\text{-TPD}$

<sup>c</sup> Fraction of Lewis acid sites as determined using pyridine adsorption (FTIR)

<sup>d</sup> First order rate constant for the double bond isomerisation of 1-butene at 373 K

on a TRISTRAR-Micromeritics apparatus. Approximately 0.25 g of the sample was degassed under N<sub>2</sub> flow at 473 K overnight prior to the measurement at 77 K.

The crystallinity of the samples was measured on an X'Pert Pro Multi Purpose Diffractometer (MPD). The diffractometer is equipped with a fast, solid state X'Celerator detector. The X-ray generator was operated at 40 kV and 40 mA, using a 1.8 kW long fine-focus cobalt tube. A programmable divergent slit of 1° was used, together with an anti-scatter slit of 2°, both in fixed mode.

The acidity of the samples was probed by ammonia desorption and pyridine adsorption. The NH<sub>3</sub>-TPD measurements were performed on a Micromeritics Autochem 2910. Prior to the NH<sub>3</sub> adsorption measurements, approximately 0.150 g of catalyst was activated at 823 K for 60 min under continuous helium flow (8.5 mL (STP)/min). The catalyst was cooled to 373 K and then saturated with ammonia in a 5% NH<sub>3</sub>/He gas mixture at the same flow rate for a period of 60 min. Physisorbed and gaseous NH<sub>3</sub> were removed by purging with helium for 30 min at 373 K. Thereafter, the sample was heated to 823 K with a heating rate of 10 K/min under a helium flow. Pyridine adsorption was used to differentiate between Lewis and Brønsted acid sites. The samples were ground to a fine powder and pressed into self-supporting wafers using a pressure of 3 tons. The wafer was dried at 773 K in vacuum for 12 h. Pyridine was adsorbed at 373 K and allowed to equilibrate for 12 min. Excess pyridine was evacuated for 1 h prior to cooling the sample to room temperature. The FTIR-spectrum of adsorbed pyridine was recorded on a Bruker Vector 22 spectrometer with air as a background. The relative amount of Lewis acid sites and Brønsted acid sites was obtained from the peaks at ca. 1450 and 1540 cm<sup>-1</sup> representing the Lewis and the Brønsted acid sites respectively, using the reported extinction coefficients [23].

The amount of coke formed on the catalyst was determined via thermo-gravimetric analysis (TGA) of the spent catalysts using a SDT 2960 Simultaneous DSC-TGA. The sample was dried at 373 K under nitrogen flow (120 mL (STP)/min). The gas environment was changed to air (120 mL (STP)/min). The sample was initially kept isothermally in this environment for 30 min. Subsequently, the temperature was raised (10 K/min) up to initially 623 K, at which temperature it was kept for 30 min, before heating the sample further to 823 K, at which temperature it was kept for a further 30 min.

### 2.3 Reaction Studies

The acidity of the support materials was further characterized using 1-butene isomerisation. The reaction was performed at 373 K and atmospheric pressure (0.85 bar) in a fixed bed reactor ( $d_{\text{reactor}} = 10 \text{ mm}$ ;  $V_{\text{catalyst}} = 2.0 \text{ ml}$ ;

GHSV = 1000 h<sup>-1</sup>). The gaseous products were collected in a sample bomb.

The metathesis of 1-butene was performed in a gas-phase fixed bed reactor [14]. The catalyst (20 mL) was activated in situ at 773 K for 16 h under a constant nitrogen flow of 20 mL (STP)/min. After activation, they were cooled down to the desired reaction temperature of 723 K. The gaseous feed (99.38 wt% 1-butene; major impurities: *n*-butane: 0.23 wt%, *cis* + *trans* 2-butene: 0.37 wt%) was led over an alumina bed to remove possible water and preheated to the reaction temperature over a bed of carborundum. The metathesis reaction was performed at atmospheric pressure (0.85 atm) and a GHSV = 425 mL (STP)/h/mL. The liquid product was collected in a catch pot and the gaseous product in the sample bomb after the reactor. The flow rate of the off-gas was measured using a wet gas flow meter.

The gaseous products were analyzed on a GC-FID equipped with a PLOT fused silica CP-Al<sub>2</sub>O<sub>3</sub>/KCl column (50 m × 530 μm × 10 μm) utilizing a temperature program (isothermal at 343 K for 3 min; ramped at a rate of 6 K/min to 463 K, and kept at this temperature for 10 min). The liquid products were analyzed on a GC-FID equipped with a CP Sil PONA column (100 m × 250 μm × 0.50 μm) utilizing a temperature program (isothermal at 323 K for 2 min; ramped at a rate of 12 K/min to 533 K, and kept at this temperature for 10 min).

### 3 Results and Discussion

Table 1 gives an overview of the support materials used in this study. γ-Al<sub>2</sub>O<sub>3</sub> consists of small γ-Al<sub>2</sub>O<sub>3</sub> crystallites with an average crystallite diameter (as estimated from XRD-line width broadening) of ca. 4 nm. Siralox-20, with a silica content of 20 wt%, consists of γ-Al<sub>2</sub>O<sub>3</sub> crystallites of the same crystal size in addition to X-ray amorphous material. Support material with a silica content larger than 20 wt% does not show any evidence of crystalline γ-Al<sub>2</sub>O<sub>3</sub>. The replacement of aluminium with silicon in the Siralox-series results in an increase in acidity. The fraction of Lewis acid sites decreases with increasing aluminium replacement by silicon. The increased number of acid sites, and most likely the increase in Brønsted acid sites, results in a strong increase in the activity of the support for the double bond isomerisation. Silica as a support does not show any noticeable evidence of acidity.

The introduction of tungsten via impregnation results in a reduction in the pore volume and to a lesser extent in the BET-surface area (cf. Tables 1, 2). The loss in pore volume must be ascribed to the adsorption of tungsten species on the support surface. The average crystallite size of γ-Al<sub>2</sub>O<sub>3</sub>, in samples with a silica content of less than 20 wt%, was

virtually unchanged. Only  $\text{WO}_3/\text{SiO}_2$  shows the presence of  $\text{WO}_3$  as a crystalline phase with an average diameter larger than 50 nm. The large crystallite size obtained in  $\text{WO}_3/\text{SiO}_2$  could have been expected [22], since the impregnation solution (at  $\text{pH} \approx 5$ ) contains negatively charged polytungstate anions [24]. Thus, an electrostatic repulsion is expected between the anions in the impregnation solution and the silica surface (iso-electric point of silica is expected to be between 1 and 2 [25]). The deposition of relatively large polytungstate anions on the silica surface during the drying process may lead to the formation of large  $\text{WO}_3$ -crystals on the silica surface. The alumina used in this study has a much higher iso-electric point of ca. 8 [26]. Thus, an electro-statically induced adsorption process may occur upon impregnating  $\gamma\text{-Al}_2\text{O}_3$  with ammonium metatungstate. Only a limited amount of tungsten can be adsorbed on an alumina support by adsorption [26]. A deposition in addition to the adsorption process [27] is probably taking place in the impregnation of alumina with ammonium metatungstate. The presence of pre-adsorbed tungstate species on the alumina surface may act as nucleation sites for the further deposition tungsten species leading to the formation of a finely dispersed tungsten phase. The point of zero-charge of silica-alumina is expected to shift to lower pH-values with increasing silica content. However, it should be realized that the surface of these materials is enriched with aluminium [28] reducing the shift in the pH value. Jara et al. [28] showed that a silica-alumina containing 63 wt%  $\text{SiO}_2$  has a IEP of 4.5. Thus, it can be expected that the electro-static adsorption of polytungstate ions on silica-alumina is reduced in comparison to alumina. It might be postulated that also in this case, the presence of some pre-adsorbed tungstate on the surface will lead to a disperse tungsten oxide phase in the catalyst.

The tungsten supported catalysts contain more acid sites than the support materials (see Table 2). Furthermore, a shift towards more Brønsted acid sites is observed. The change in the acidity due to the introduction of tungsten on the support is best viewed by looking at the difference of the  $\text{NH}_3$ -TPD-profile of the supported  $\text{WO}_3$ -catalysts

and the TPD-profile of the support (see Fig. 2). The impregnation of ammonium metatungstate on  $\gamma\text{-Al}_2\text{O}_3$  results in a decrease in the number of acid sites desorbing ammonia between 500 and 570 K and an increase in the number of acid sites desorbing ammonia between 580 and 780 K. Hence, the introduction of tungsten on alumina leads to the generation of more strongly adsorbing sites. Similar conclusions were derived for a DFT-study on the acidity of Mo–O–Al clusters compared to the acidity of Al–O–Al-clusters [29].

Tungsten supported on silica-alumina also results in an increase in number of acid sites and in particular to sites desorbing at temperatures larger than 430 K. Silica does virtually not adsorb ammonia, whereas  $\text{WO}_3/\text{SiO}_2$  shows acidity [4] through ammonia desorption with a peak

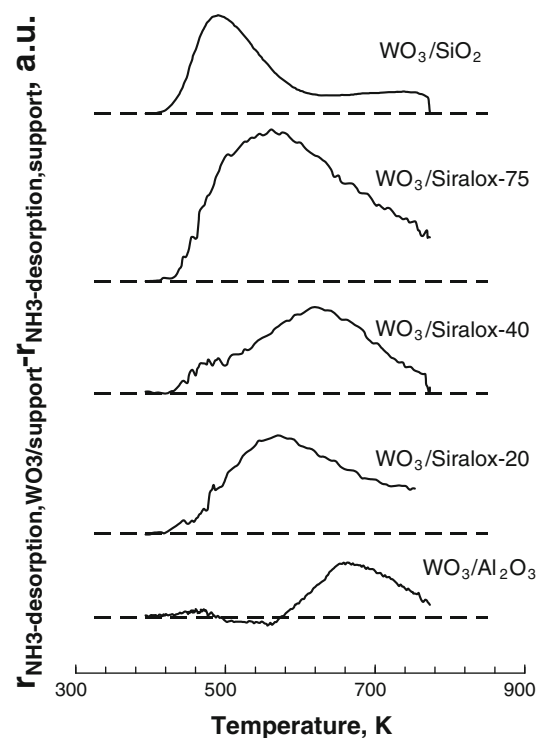


**Fig. 2** Difference of the  $\text{NH}_3$ -TPD-profile of tungsten supported on alumina, Siralox and silica and their support material

**Table 2** Characteristics of supported tungsten catalysts

Catalyst	$S_{\text{BET}}$ ( $\text{m}^2/\text{g}$ )	$V_{\text{Pore}}$ ( $\text{cm}^3/\text{g}$ )	$d_{\text{pore}}$ ( $\text{\AA}$ )	$d_{\text{Al}_2\text{O}_3}$ ( $\text{\AA}$ )	$d_{\text{WO}_3}$ ( $\text{\AA}$ )	$n_{\text{acid}}^{\text{a}}$ (mmol/g)	$x_{\text{Lewis}}^{\text{b}}$
8 wt% $\text{WO}_3/\gamma\text{-Al}_2\text{O}_3$	237	0.70	119	47	—	0.23	100
8 wt% $\text{WO}_3/\text{Siralox}$ 20	311	0.63	81	42	—	0.29	90
8 wt% $\text{WO}_3/\text{Siralox}$ 40	328	0.75	92	—	—	0.33	78
8 wt% $\text{WO}_3/\text{Siralox}$ 75	246	0.25	41	—	—	0.37	69
8 wt% $\text{WO}_3/\text{SiO}_2$	260	1.02	156	—	>500	0.05	99

<sup>a</sup> Number of acid sites as determined using  $\text{NH}_3$ -TPD

<sup>b</sup> Fraction of Lewis acid sites as determined using pyridine adsorption (FTIR)

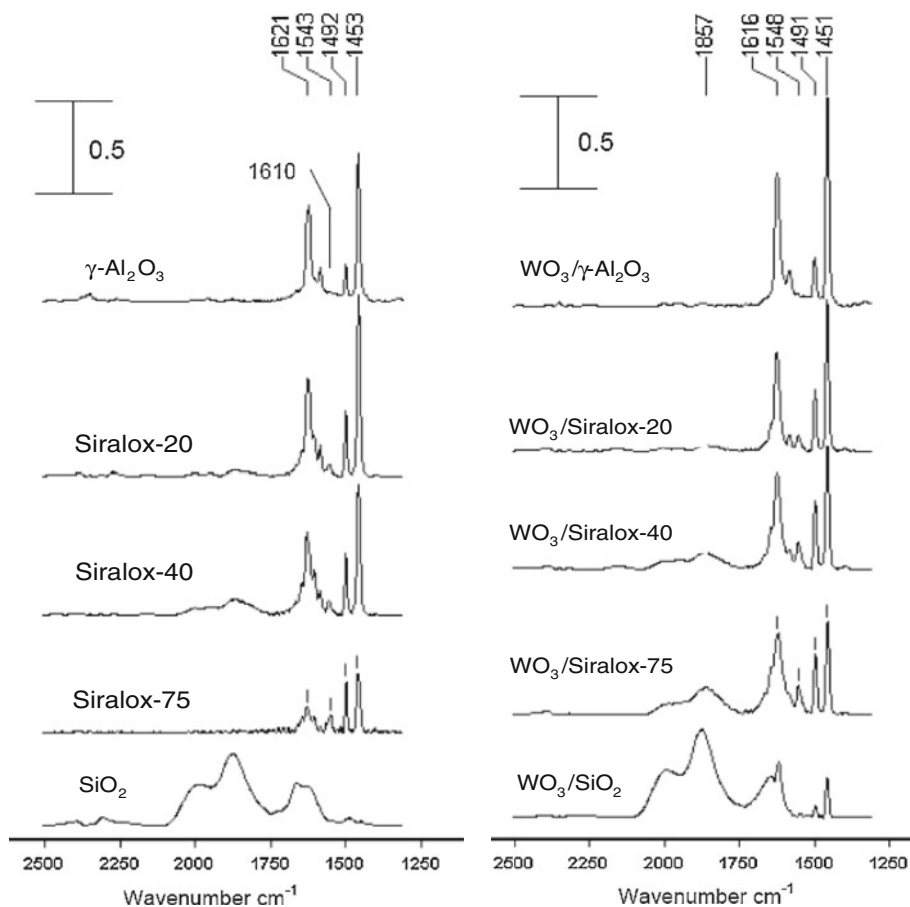
maximum at 490 K. It can thus be concluded that the  $\text{WO}_3/\text{SiO}_2$  has not only less acid sites, but also weaker acid sites, than  $\text{WO}_3/\gamma\text{-Al}_2\text{O}_3$ . The additional sites introduced by tungsten impregnated on silica-alumina (Siralox) seem to have an acid strength between  $\text{WO}_3/\text{SiO}_2$  and  $\text{WO}_3/\gamma\text{-Al}_2\text{O}_3$  with peak maximums between 550 and 625 K. This might be attributed to the direct contact of  $\text{WO}_3$  with either alumina or silica type of sites.

FTIR of adsorbed pyridine was used to study the Brønsted and Lewis acidity of the range of supports and the corresponding supported tungsten catalysts (see Fig. 3). The characteristic bands of pyridine protonated by Brønsted acid sites (pyridinium ions) appearing at  $\sim 1543$  and  $1640 \text{ cm}^{-1}$  and bands from pyridine coordinated to Lewis acid sites appearing at ca.  $1453$  and  $1621 \text{ cm}^{-1}$ . The peak appearing at  $1621 \text{ cm}^{-1}$  is associated with Lewis acid sites in the tetrahedral coordination, while the small peak beside it at  $1612 \text{ cm}^{-1}$  is due to Lewis acid sites in the octahedral environment [30]. The peak appearing at  $1453 \text{ cm}^{-1}$  represents the total amount of Lewis acid sites in the tetrahedral and octahedral environment. The peak associated with the band appearing at  $1543 \text{ cm}^{-1}$ , is accompanied by the vibration of the pyridinium ion resulting from the protonation of pyridine by Brønsted acid sites.

Brønsted acid sites ( $1545 \text{ cm}^{-1}$ ) are absent for  $\gamma\text{-Al}_2\text{O}_3$  and  $\text{SiO}_2$  and only present in samples containing silica as well as alumina. The modification of  $\text{Al}_2\text{O}_3$  with silica led to the creation of both highly acidic Lewis and Brønsted acid sites, as previously observed for silica-alumina [30]. Lewis acid sites are created via the isomorphous substitution of  $\text{Si}^{4+}$  by  $\text{Al}^{3+}$  ions at tetrahedral lattice sites and Brønsted acid sites via the formation of bridged hydroxyl groups.

The FTIR-spectra of the tungsten-impregnated supports show bands at  $1451 \text{ cm}^{-1}$  which corresponds to pyridine coordinated to Lewis acid sites. This peak represents the total amount of Lewis acid sites. The peaks appearing at  $1548 \text{ cm}^{-1}$  indicate the presence of pyridinium ions originating from pyridine protonated by Brønsted acid sites. These bands were only observed with catalysts containing 20, 40, 75 wt% silica. For the pure alumina supported tungsten, no such peak was observed. The peak at  $1491 \text{ cm}^{-1}$ , is accompanied by the vibration of the pyridinium ion. Pure silica does not contain any Lewis or Brønsted acid sites. However, an adsorption band at  $1449 \text{ cm}^{-1}$  is observed for  $\text{WO}_3/\text{SiO}_2$ . This represents the Lewis acidity of  $\text{WO}_3/\text{SiO}_2$  and is thus due to the Lewis acidity of tungsten impregnated on to the support. Hence,

**Fig. 3** FTIR-spectra of the pyridine adsorbed on the support materials (left) and on tungsten supported on the support materials (right)



the peaks appearing at  $1449\text{ cm}^{-1}$  for all support materials must be ascribed due to pyridine coordinated to all Lewis acid sites, i.e. Lewis sites present on the support and the Lewis acid sites induced by tungsten present on the support. The strength of the Lewis acid sites, typically observed by a shift in peak, has not been noticeably affected by the introduction of tungsten on to the support. However, tungsten on the support resulted in an increase in the total acidity of the catalyst.

The primary metathesis reaction is equilibrium limited, and a maximum conversion of  $n\text{-C}_4\text{-olefins}$  of ca. 71% is achievable at a reaction temperature of 723 K.  $\text{WO}_3/\text{SiO}_2$  shows an almost constant activity as a function of time-on-line close to the equilibrium conversion of the primary metathesis reaction (see Fig. 4). It should however be noted that the double bond isomerisation over  $\text{WO}_3/\text{SiO}_2$  is not at equilibrium (in contrast to the double bond isomerisation over the other catalysts), since the 2-butene content in the fraction of linear butenes is only ca. 44 mol% (at equilibrium a 2-butene content in the fraction of linear butenes should be ca. 73 mol%). This implies that the primary metathesis reaction over  $\text{WO}_3/\text{SiO}_2$  is not at equilibrium.

A higher conversion of the  $n\text{-C}_4\text{-olefins}$  than expected if the primary metathesis reaction is equilibrium limited was obtained over tungsten supported on Siralox-75 and on Siralox-40 implying that the primary metathesis reaction is not the sole reaction taking place.  $\text{WO}_3/\text{Siralox-20}$  and  $\text{WO}_3/\gamma\text{-Al}_2\text{O}_3$  showed a much lower activity. It can be further noted that all catalysts except  $\text{WO}_3/\text{SiO}_2$  show a decline in activity with time-on-line. The decline in the catalyst activity, as defined by the apparent first order rate constant for the conversion of  $n\text{-C}_4\text{-olefins}$  after 6 h on line relative to the apparent first order rate constant after 1 h on line becomes less with increasing silica content in the

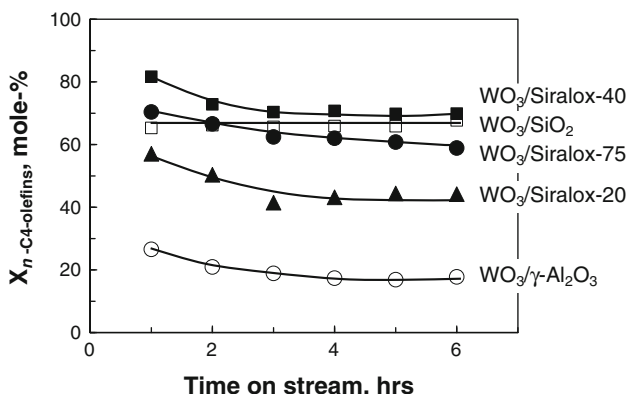


**Fig. 4** Conversion of  $n\text{-butenes}$  in the metathesis over supported tungsten catalysts (open circle:  $\text{WO}_3/\text{Al}_2\text{O}_3$ ; filled triangle:  $\text{WO}_3/\text{Siralox-20}$ ; filled square:  $\text{WO}_3/\text{Siralox-40}$ ; filled circle:  $\text{WO}_3/\text{Siralox-75}$ ; open square:  $\text{WO}_3/\text{SiO}_2$ )

support material, i.e.  $\text{WO}_3/\gamma\text{-Al}_2\text{O}_3 > \text{WO}_3/\text{Siralox-20} > \text{WO}_3/\text{Siralox-40} > \text{WO}_3/\text{Siralox-75} > \text{WO}_3/\text{SiO}_2$ . The decline in catalyst activity cannot be correlated directly with either the number of acid sites or with the strength of acid sites in the catalyst.

The selectivity of the primary metathesis product, ethene, is typically lower than equilibrium selectivity for the primary metathesis reaction (see Fig. 5), with the exception of the selectivity obtained with  $\text{WO}_3/\text{SiO}_2$ . The ratio of ethene to  $C_6$ -olefins decreases with increasing time-on-line, and is in the product obtained over  $\text{WO}_3/\text{SiO}_2$  higher than expected for the primary metathesis reaction (ca.  $1.6 \pm 0.1$  mol ethene/mol  $C_6$ -olefins) indicating secondary metathesis reactions resulting in ethene formation. The products obtained over  $\text{WO}_3/\text{Siralox-40}$  show a ratio of ethene to  $C_6$ -olefins significantly lower than the expected ratio of the primary metathesis reaction ( $0.66 \pm 0.03$  mol ethene/mol  $C_6$ -olefins). The selectivity for the other primary metathesis product propene (assuming a rapid equilibration between  $n\text{-C}_4\text{-olefins}$ ) is typically higher than the equilibrium selectivity as predicted for the primary metathesis reaction. This indicates that other

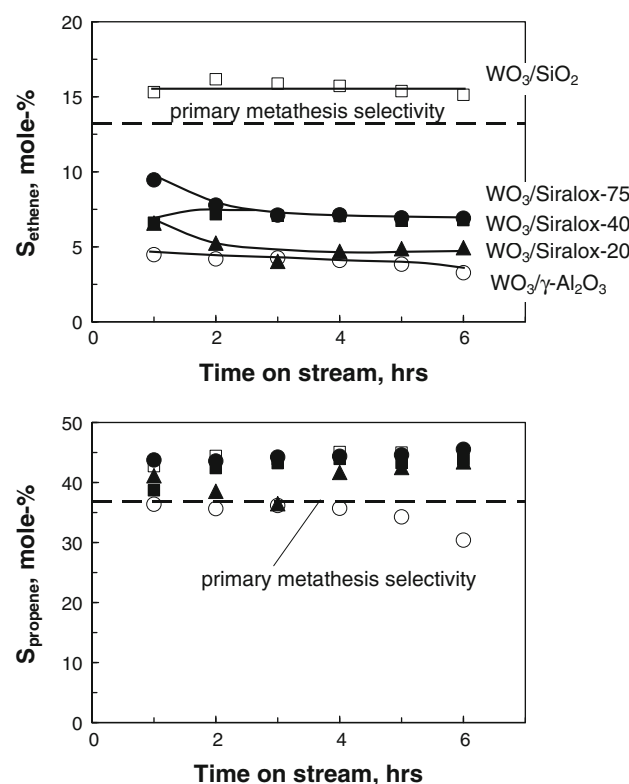


**Fig. 5** Molar selectivity for primary metathesis products (top: ethene; bottom: propene) in the metathesis of  $n\text{-butenes}$  over supported tungsten (open circle:  $\text{WO}_3/\text{Al}_2\text{O}_3$ ; filled triangle:  $\text{WO}_3/\text{Siralox-20}$ ; filled square:  $\text{WO}_3/\text{Siralox-40}$ ; filled circle:  $\text{WO}_3/\text{Siralox-75}$ ; open square:  $\text{WO}_3/\text{SiO}_2$ ; dotted line equilibrium selectivity for the primary metathesis reaction)

reactions result in the formation of propene as well. Furthermore, the molar ratio of propene to C<sub>5</sub>-olefins is much larger than 1 ranging from 1.5 to 1.6 for the silica-rich catalysts going down to 1.4 ± 0.1 for the molar ratio of propene to C<sub>5</sub>-olefins obtained over WO<sub>3</sub>/Siralox-20 and 1.12 ± 0.06 for the ratio obtained over WO<sub>3</sub>/γ-Al<sub>2</sub>O<sub>3</sub>. The higher than expected selectivity for the primary metathesis product propene (and to some extent of ethene) compared to the selectivity of the corresponding long chain olefins might originate from the secondary metathesis reactions involving butenes yielding even longer chain product compounds. However, it should be noted that the selectivity for the longer chain products (lumped together as C<sub>7+</sub>—see Table 3) is rather low (3–13 C%) and can only partially explain the high propene selectivity.

Coke formation is typically observed in the metathesis over supported tungsten catalysts [19, 20]. Coke formation was observed over all catalyst (with exception of WO<sub>3</sub>/SiO<sub>2</sub>) in the limited run time of these experiments (see Fig. 6). Coke formation was enhanced over the catalyst WO<sub>3</sub>/Siralox-40, and could be related to the acidity of the support for the silica-alumina supports (Siralox-series). It should however be noted that the amount of coke formed could not be correlated directly to the amount of catalyst deactivation. This implies that at least some of the coke formed is located on the support and does not interfere with the metathesis reaction. Coke is thought to be hydrogen poor, and thus the product effluent should contain more hydrogen than the feed (see Table 3). This can be in the form of paraffinic compounds. Some paraffins are found in each carbon number fraction. The paraffin selectivity passes a maximum as a function of the silica content in the support material at a silica content of 20 wt% implying that the acidity of the support does play a role in the

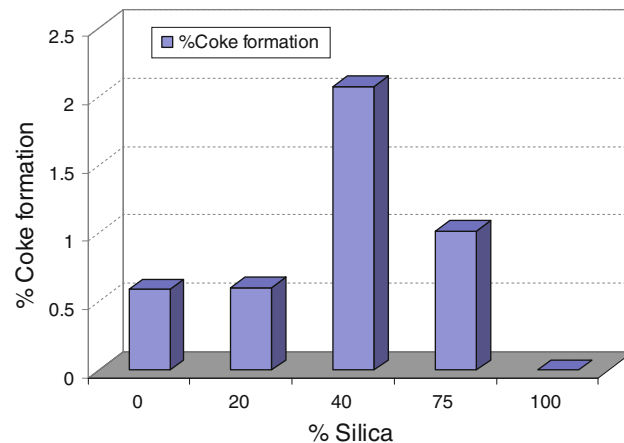


**Fig. 6** Coke formation reported as weight loss in the oxidative treatment of the spent catalyst in the metathesis of *n*-butenes over supported tungsten

dehydrogenation of the coke precursor. Coke formation can be accompanied with methane formation through demethylation. However, the methane selectivity is typically less than 0.2 mol%. This is thus not a major reaction pathway under metathesis reaction conditions. The total selectivity for C<sub>2</sub>–C<sub>5</sub>-paraffins amounted to between 0.1 and 3.5 mol% implying that the pairing reaction [31] plays some role in the formation of hydrogen-poor surface species.

The selectivity of branched product compounds, and especially iso-butene, is rather high (see Table 3), although much lower than in thermodynamic equilibrium under these conditions. The formation of branched isomers may occur through an acid catalysed, skeletal isomerisation, and it can be best evaluated by considering the amount of branched, olefinic isomers in the fraction of olefins of a particular carbon number (see Fig. 7). Their formation was

**Table 3** Performance of supported 8 wt% WO<sub>3</sub>-catalysts in the *n*-butene metathesis (T = 723 K, p = 0.85 bar; GHSV = 425 mL (STP)/h/mL) after 6 h on line

	WO <sub>3</sub> /γ-Al <sub>2</sub> O <sub>3</sub>	WO <sub>3</sub> /Siralox-20	WO <sub>3</sub> /Siralox-40	WO <sub>3</sub> /Siralox-75	WO <sub>3</sub> /SiO <sub>2</sub>
X <sub>n-C<sub>4</sub>-olefins</sub> (mol%)	17.8	44.2	58.9	69.9	67.7
(H <sub>2</sub> /C) <sub>product</sub> (mol/mol)	2.01	2.02	2.01	2.00	2.00
S <sub>CH<sub>4</sub></sub> (C%)	0.1	0.2	0.0	0.0	0.0
S <sub>C<sub>7+</sub></sub> (C%)	9.6	3.8	2.8	12.2	5.7
S <sub>ethene</sub> (mol%)	3.3	4.9	6.8	6.9	15.1
S <sub>ethane</sub> (mol%)	0.0	0.3	0.1	0.1	0.0
S <sub>propene</sub> (mol%)	30.2	42.7	43.9	45.3	43.7
S <sub>propane</sub> (mol%)	0.0	0.8	0.2	0.4	0.0
S <sub>n-butane</sub> (mol%)	0.7	1.8	0.0	0.6	0.0
S <sub>iso-butene</sub> (mol%)	26.8	10.5	5.3	6.7	0.3
S <sub>1-pentene</sub> (mol%)	2.3	2.3	2.2	2.4	6.0
S <sub>2-pentenes</sub> (mol%)	11.1	10.7	15.1	11.9	20.9
S <sub>n-pentane</sub> (mol%)	0.8	0.6	0.1	0.5	0.1
S <sub>iso-C<sub>5</sub></sub> (mol%)	15.1	17.1	8.9	16.6	0.4
S <sub>C<sub>6</sub></sub> (mol%)	4.2	5.6	10.6	7.0	10.3

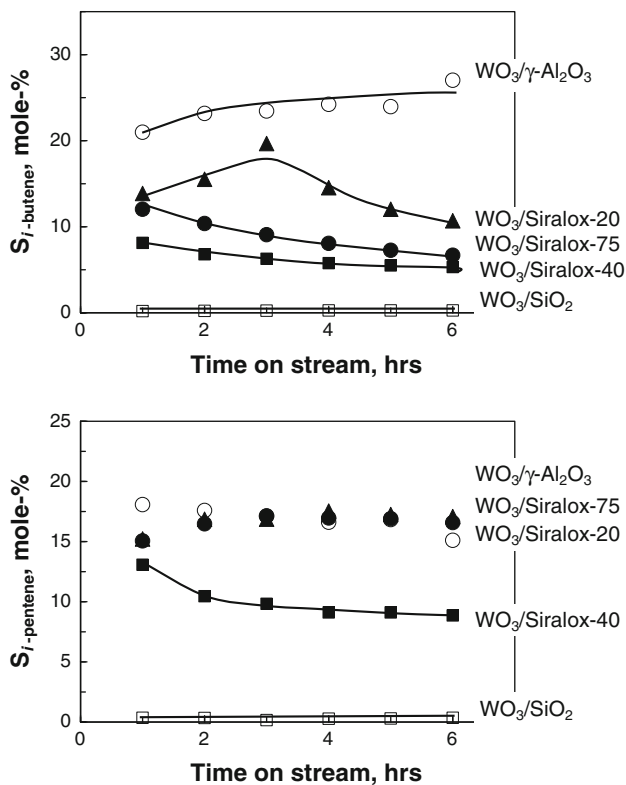


**Fig. 7** Molar selectivity for the formation of branched product compounds (iso-butene: top; iso-pentene: bottom) in the metathesis of *n*-butenes over supported tungsten (open circle: WO<sub>3</sub>/Al<sub>2</sub>O<sub>3</sub>; filled triangle: WO<sub>3</sub>/Siralox-20; filled square: WO<sub>3</sub>/Siralox-40; filled circle: WO<sub>3</sub>/Siralox-75; open square: WO<sub>3</sub>/SiO<sub>2</sub>)

previously related to Brønsted acidity within the catalyst [22], since they only appear at higher tungsten loadings, and can be suppressed by poisoning the acid sites with potassium. All catalysts, with the exception of WO<sub>3</sub>/SiO<sub>2</sub>, show a large extent of skeletal isomerisation, although the skeletal isomerisation is not at equilibrium. The formation of iso-pentene seems to be loosely correlated with the acidity of the catalyst, with catalyst based on the alumina containing support material showing a higher acidity and a higher selectivity towards iso-pentene.

This seems however not to be the case, for the selectivity of iso-butene, although the iso-butene content in the fraction of C<sub>4</sub>-olefins follows a similar trend. The highest selectivity was obtained with the least active catalyst, viz. WO<sub>3</sub>/Al<sub>2</sub>O<sub>3</sub> (ca. 27–30 mol%), but the relative large amount of *n*-C<sub>4</sub>-olefins present in the effluent results in a low ratio of iso-butene in the fraction of C<sub>4</sub>-olefins (0.05 mol/mol). The obtained ratio of iso-butene in the fraction of C<sub>4</sub>-olefins over WO<sub>3</sub> supported on silica-alumina is higher (ca. 0.08–0.10 mol/mol), although the selectivity for iso-butene is much reduced (5–15 mol%). Metathesis of *n*-butenes over WO<sub>3</sub>/SiO<sub>2</sub> does not lead noticeably to the formation of iso-butene (S<sub>iso</sub>-butene < 0.3 mol%). The selectivity of iso-butene is

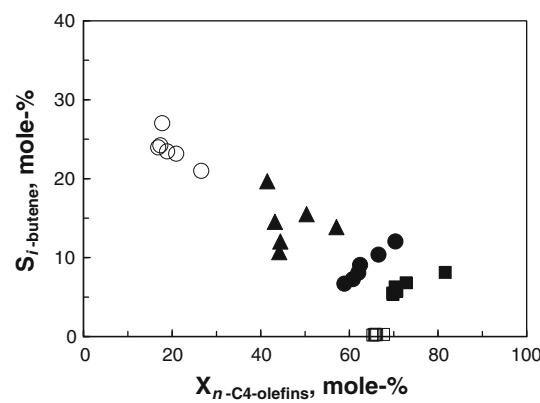


**Fig. 8** Molar selectivity for iso-butene as a function of the obtained conversion level (open circle: WO<sub>3</sub>/Al<sub>2</sub>O<sub>3</sub>; filled triangle: WO<sub>3</sub>/Siralox-20; filled square: WO<sub>3</sub>/Siralox-40; filled circle: WO<sub>3</sub>/Siralox-75; open square: WO<sub>3</sub>/SiO<sub>2</sub>)

lower over catalyst with a high activity and high over catalysts with a low activity (see Fig. 8). The metathesis of 1-butene is presumably taking place over low coordination tungsten sites, since they are expected to be more stable than the high coordination sites [29]. The coordination of an adsorbed olefin to a low coordination tungsten atom may result in the formation of a surface alkoxide species leading to double bond isomerisation. The further interaction of the low coordination tungsten atom with an olefin may result in the formation of an iso-C<sub>8</sub>-alkoxy-species. Intramolecular skeletal isomerisation of the adsorbed iso-C<sub>8</sub>-alkoxide-species and subsequent splitting into C<sub>4</sub>-fragments may lead to the formation of iso-butene. Similar reaction schemes are well known in acid catalysed reactions [32]. The likelihood for this type of reactions is expected to increase with increasing strength of the acidity of the hydroxyl-group(s) on the surface tungsten complex, i.e. with increasing W–O–Al interaction, but also with increasing size of the surface tungsten complex [29]. Furthermore, the association of the surface tungsten site with branched C<sub>8</sub>-alkoxide species will result in steric hindrance for the coordination of olefins to the low coordination tungsten site for further reaction. Strong acid sites are expected to adsorb olefins more strongly thus resulting in reduced activity on the tungsten site due to geometric constraint at the site. Hence, 1-butene metathesis over WO<sub>3</sub>/γ-Al<sub>2</sub>O<sub>3</sub> results in a relatively large selectivity to iso-butene and a low activity.

The C<sub>5</sub>-fraction does not only contain linear C<sub>5</sub>-products and their skeletal isomerisation products, but also cyclopentenes. Cyclic compounds are thought to be related to coke formation. The selectivity for these products is particularly high on catalysts, with strong acid sites present due to the incorporation of tungsten on the support material. Coke formation correlates with yield of these compounds, i.e. a high activity and a high selectivity are required for the formation of coke. For instance WO<sub>3</sub>/γ-

$\text{Al}_2\text{O}_3$  shows a high selectivity for these compounds, but the overall activity is reduced (presumably due to steric hindrance at the activity sites resulting from the formation of bulky alkoxy-compounds).

#### 4 Conclusions

The metathesis of *n*-butenes over supported tungsten catalysts over supported tungsten catalysts yields in addition to the expected primary metathesis products with relative selectivity iso-butene. The reaction sequence taking place on the catalyst surface is more complex than the reaction scheme following the primary metathesis reaction. It was shown that the formation of short chain olefins is in abundance in relation to the formation of the corresponding long chain product compounds. This might (partially) result from secondary metathesis reactions taking place yielding in the formation of long chain olefinic products.

The metathesis of 1-butene yielded a relative large amount of iso-butene. The selectivity of iso-butene seems to be inversely related to the activity of the catalysts. This was ascribed to the formation of bulky iso-alkoxide species restricting access to the active tungsten species and thus resulting in a diminished catalyst activity. It is argued that the formation of the branched iso-alkoxide species requires strong acid sites as present in tungsten species associated with alumina.

Coke formation requires a relative high activity and a high selectivity for coke precursors (typically formed by acid catalysed reactions). A pairing reaction may result in the dehydrogenation of the coke precursor accompanied by the formation of paraffinic compounds.

#### References

1. Claeys M, van Steen E (2004) Stud Surf Sci Catal 152:601–680
2. Mol JC (2004) J Mol Catal A 213:39–45
3. Huang S, Liu S, Xin W, Bai J, Xie S, Wang Q, Xu L (2005) J Mol Catal A 226:61–68
4. Wang Y, Chen Q, Yang W, Xie Z, Xu W, Huang D (2003) Appl Catal A 250:25–37
5. Stull DR, Westrum EF, Sinke GC (1969) The chemical thermodynamics of organic compounds. Wiley, New York
6. Zhao Q, Chen S-L, Gao J, Xu C (2009) Transit Met Chem 34:621
7. Ivin KJ, Mol JC (1997) Olefin metathesis and metathesis polymerization, vol 2. Academic Press, San Diego, p 25
8. Andreini A, Xu X, Mol JC (1986) Appl Catal 27:31–40
9. Sibeijn M, Mol JC (1991) Appl Catal 67:279–295
10. Balcar H, Hamtil R, Žilková N, Čejka J (2004) Catal Lett 97:25
11. Oikawa T, Ookoshi T, Tanaka T, Yamamoto T, Onanka M (2004) Microporous Mesoporous Mater 74:93
12. Aguado J, Escola JM, Castro MC, Paredes B (2005) Appl Catal A 284:47
13. Hamtil R, Žilková N, Balcar H, Čejka J (2006) Appl Catal A 302:193
14. Topka P, Balcar H, Rathousky J, Žilková N, Verpoort F, Čejka J (2006) Microporous Mesoporous Mater 96:44
15. Bakala PC, Briot E, Millot Y, Piqumal J-Y, Brégeault JM (2008) J Catal 258:61
16. van Roosmalen AJ, Mol JC (1980) J Chem Soc Chem Commun 704
17. Adreine A, Mol JC (1985) J Chem Soc Faraday Trans I 81:1705
18. van Roosmalen AJ, Kosterm D, Mol JC (1980) J Phys Chem 84:3075–3079
19. Spamer A, Dube TI, Moodley DJ, van Schalkwyk C, Botha JM (2003) Appl Catal A 255:133–142
20. van Schalkwyk C, Spamer A, Moodley DJ, Dube T, Reynhardt J, Botha JM (2003) Appl Catal A 255:121–131
21. Bartholomew CH (2001) Appl Catal A 212:17–60
22. Spamer A, Dube TI, Moodley DJ, van Schalkwyk C, Botha JM (2003) Appl Catal A 255:153–167
23. Emeis CA (1993) J Catal 141:347–354
24. Panagiotou GD, Petsi T, Bourikas K, Kordulis C, Lycourghiotis A (2009) J Catal 262:266–279
25. Parks GA, de Bruyn PL (1962) J Phys Chem 66:967–973
26. Knözinger H, Taglauer E (1993) Catalysis 10:1
27. van Steen E, Viljoen EL, van de Loosdrecht J, Claeys M (2008) Appl Catal A 335:56–63
28. Jara AA, Goldberg S, Mora ML (2005) J Colloid Interface Sci 292:160–170
29. van Steen E, Viljoen EL, Claeys M (2007) J Mol Catal A 266:254–259
30. Rajagopal S, Marzari JA, Miranda R (1995) J Catal 151:192
31. Röger HP, Böhrieger W, Möller KP, O'Connor CT (2000) Stud Surf Sci Catal 130:281
32. Ramani NC, Sullivan DL, Ekerdt JG (1998) J Catal 173:105